THE ASTROPHYSICAL JOURNAL, 497:L17–L20, 1998 April 10
© 1998. The American Astronomical Society. All rights reserved. Printed in U.S.A.

SPECTRA AND LIGHT CURVES OF GAMMA-RAY BURST AFTERGLOWS

RE'EM SARI,[1] TSVI PIRAN,[1] AND RAMESH NARAYAN[2]
Received 1997 December 1; accepted 1998 February 9; published 1998 March 11

ABSTRACT

The recently discovered gamma-ray burst afterglow is believed to be described reasonably well by synchrotron emission from a decelerating relativistic shell that collides with an external medium. To compare theoretical models with afterglow observations, we calculate here the broadband spectrum and corresponding light curve of synchrotron radiation from a power-law distribution of electrons in an expanding relativistic shock. Both the spectrum and the light curve consist of several power-law segments with related indices. The light curve is constructed under two limiting models for the hydrodynamic evolution of the shock: fully adiabatic and fully radiative. We give explicit relations between the spectral index and the temporal power-law index. Future observations should be able to distinguish between the possible behaviors and determine the type of solution.

Subject headings: gamma rays: bursts — hydrodynamics — relativity — shock waves

1. INTRODUCTION

Delayed emission in X-ray, optical, and radio wavelengths has been seen recently in a few gamma-ray bursts (GRBs) (Costa et al. 1997; Groot et al. 1997; Frail et al. 1997). This "afterglow" is described reasonably well as synchrotron emission from accelerated electrons when a spherical relativistic shell collides with an external medium (Paczyński & Rhoads 1993; Katz 1994; Waxman 1997a, 1997b; Wijers, Rees, & Mészáros 1997; Katz & Piran 1997a; Mészáros, Rees, & Wijers 1997). Previous analyses described the spectrum and light curve only over a limited range of frequencies and time. In this Letter, we discuss the spectrum over a wide range of frequencies and derive the light curve from very early to late times. We focus on the optical and X-ray emission, where synchrotron self-absorption is not important, and we assume that the shell is ultrarelativistic. We allow for both adiabatic and radiative hydrodynamic evolution.

Consider a relativistic shock propagating through a uniform cold medium with particle density n. Behind the shock, the particle density and the energy density are given by $4\gamma n$ and $4\gamma^2 n m_p c^2$, respectively, where γ is the Lorentz factor of the shocked fluid (Blandford & McKee 1976). We assume that electrons are accelerated in the shock to a power-law distribution of Lorentz factor γ_e, with a minimum Lorentz factor γ_m: $N(\gamma_e)d\gamma_e \propto \gamma_e^{-p} d\gamma_e$, $\gamma_e \geq \gamma_m$. To keep the energy of the electrons finite, we take $p > 2$. We assume that a constant fraction ϵ_e of the shock energy goes into the electrons. Then

$$\gamma_m = \epsilon_e \left(\frac{p-2}{p-1}\right) \frac{m_p}{m_e} \gamma \cong 610 \epsilon_e \gamma, \tag{1}$$

where the coefficient on the right corresponds to the standard choice, $p = 2.5$ (Sari, Narayan, & Piran 1996). We also assume that the magnetic energy density behind the shock is a constant fraction ϵ_B of the shock energy. This gives a magnetic field strength (fluid frame)

$$B = (32\pi m_p \epsilon_B n)^{1/2} \gamma c. \tag{2}$$

We consider only synchrotron emission and ignore inverse Compton scattering, which is important when $\epsilon_B > \epsilon_e$.

2. SYNCHROTRON SPECTRUM OF A RELATIVISTIC SHOCK

The radiation power and the characteristic synchrotron frequency from a randomly oriented electron with Lorentz factor $\gamma_e \gg 1$ in a magnetic field B are

$$P(\gamma_e) = \frac{4}{3} \sigma_T c \gamma^2 \gamma_e^2 \frac{B^2}{8\pi}, \tag{3}$$

$$\nu(\gamma_e) = \gamma \gamma_e^2 \frac{q_e B}{2\pi m_e c}. \tag{4}$$

The factors of γ^2 and γ are introduced to transform the results from the frame of the shocked fluid to the frame of the observer. The spectral power, P_ν (power per unit frequency, in units of ergs Hz^{-1} s^{-1}), varies as $\nu^{1/3}$ for $\nu < \nu(\gamma_e)$ and cuts off exponentially for $\nu > \nu(\gamma_e)$. The peak spectral power occurs at $\nu(\gamma_e)$:

$$P_{\nu,\max} \approx \frac{P(\gamma_e)}{\nu(\gamma_e)} = \frac{m_e c^2 \sigma_T}{3 q_e} \gamma B, \tag{5}$$

and it is independent of γ_e.

The above description of P_ν is suitable when the electron does not lose a significant fraction of its energy to radiation. This requires γ_e to be less than a critical value γ_c given by $\gamma \gamma_c m_e c^2 = P(\gamma_c) t$:

$$\gamma_c = \frac{6\pi m_e c}{\sigma_T \gamma B^2 t} = \frac{3 m_e}{16 \epsilon_B \sigma_T m_p c} \frac{1}{t \gamma^3 n}, \tag{6}$$

where t refers to time in the frame of the observer.

An electron with an initial Lorentz factor $\gamma_e > \gamma_c$ cools down to γ_c in the time t. As it cools, the frequency of the synchrotron emission varies as $\nu \propto \gamma_e^2$, while the electron energy varies as γ_e. It then follows that the spectral power varies as $\nu^{-1/2}$ over the frequency range $\nu_c < \nu < \nu(\gamma_e)$, where we have defined $\nu_c \equiv \nu(\gamma_c)$. The net spectrum of radiation from such an electron then consists of three segments: a low-energy tail for $\nu < \nu_c$, where P_ν goes as $\nu^{1/3}$; a power-law segment between ν_c and

[1] The Racah Institute of Physics, The Hebrew University, Jerusalem 91904, Israel; sari@nikki.fiz.huji.ac.il, tsvi@nikki.fiz.huji.ac.il.
[2] Harvard-Smithsonian Center for Astrophysics, 60 Garden Street, Cambridge, MA 02138; narayan@surya.harvard.edu.

$\nu(\gamma_e)$, where $P_\nu \sim \nu^{-1/2}$; and an exponential cutoff for $\nu > \nu(\gamma_e)$. The maximum emissivity occurs at ν_c and is given by $P_{\nu,\max}$.

To calculate the net spectrum from a power-law distribution of electrons, we need to integrate over γ_e. There are now two different cases, depending on whether $\gamma_m > \gamma_c$ or $\gamma_m < \gamma_c$.

Let the total number of swept-up electrons in the postshock fluid be $N_e = 4\pi R^3 n/3$. When $\gamma_m > \gamma_c$, all the electrons cool down to roughly γ_c, and the spectral power at ν_c is approximately $N_e P_{\nu,\max}$. We call this the case of *fast cooling*. The flux at the observer, F_ν, is given by

$$F_\nu = \begin{cases} (\nu/\nu_c)^{1/3} F_{\nu,\max}, & \nu_c > \nu, \\ (\nu/\nu_c)^{-1/2} F_{\nu,\max}, & \nu_m > \nu > \nu_c, \\ (\nu_m/\nu_c)^{-1/2} (\nu/\nu_m)^{-p/2} F_{\nu,\max}, & \nu > \nu_m, \end{cases} \tag{7}$$

where $\nu_m \equiv \nu(\gamma_m)$ and $F_{\nu,\max} \equiv N_e P_{\nu,\max}/4\pi D^2$ is the observed peak flux at distance D from the source.

When $\gamma_c > \gamma_m$, only those electrons with $\gamma_e > \gamma_c$ can cool. We call this *slow cooling*, because the electrons with $\gamma_e \sim \gamma_m$, which form the bulk of the population, do not cool within a time t, and we have

$$F_\nu = \begin{cases} (\nu/\nu_m)^{1/3} F_{\nu,\max}, & \nu_m > \nu, \\ (\nu/\nu_m)^{-(p-1)/2} F_{\nu,\max}, & \nu_c > \nu > \nu_m, \\ (\nu_c/\nu_m)^{-(p-1)/2} (\nu/\nu_c)^{-p/2} F_{\nu,\max}, & \nu > \nu_c. \end{cases} \tag{8}$$

The typical spectra corresponding to fast and slow cooling are shown in Figures 1*a* and 1*b*. The low-energy part of these spectra has empirical support even within the GRB itself (Cohen et al. 1997). In addition to the various power-law regimes described above, self-absorption causes a steep cutoff of the spectrum at low frequencies (Katz 1994; Waxman 1997b; Katz & Piran 1997a). For completeness, we show this regime in Figure 1, but we shall ignore it for the rest of this Letter since it does not affect either the optical or the X-ray radiation in which we are interested.

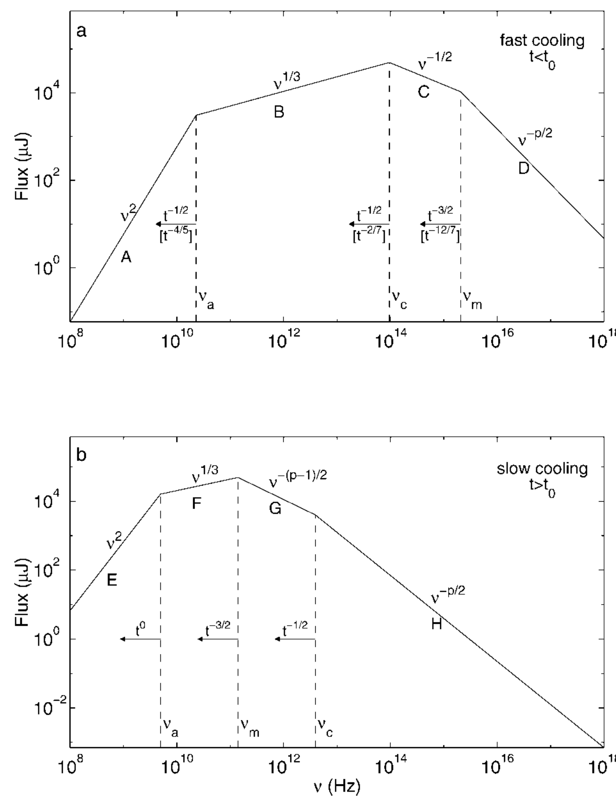

FIG. 1.—Synchrotron spectrum of a relativistic shock with a power-law electron distribution. (*a*) Fast cooling, which is expected at early times ($t < t_0$). The spectrum consists of four segments, identified as A, B, C, and D. Self-absorption is important below ν_a. The frequencies, ν_m, ν_c, and ν_a, decrease with time as indicated; the scalings above the arrows correspond to an adiabatic evolution, and the scalings below, in square brackets, correspond to a fully radiative evolution. (*b*) Slow cooling, which is expected at late times ($t > t_0$). The evolution is always adiabatic. The four segments are identified as E, F, G, and H.

3. HYDRODYNAMIC EVOLUTION AND LIGHT CURVES

The instantaneous spectra do not depend on the hydrodynamic evolution of the shock. The *light curves* at a given frequency, however, depend on the temporal evolution of various quantities, such as the break frequencies ν_m and ν_c and the peak flux $F_{\nu,\max}$. These depend, in turn, on how γ and N_e scale as a function of t.

We limit the discussion here to a spherical shock of radius $R(t)$ propagating into a constant surrounding density n. We consider two extreme limits for the hydrodynamic evolution of the shock: either fully radiative or fully adiabatic. In a radiative evolution, all the internal energy generated in the shock is radiated. This requires two conditions to be satisfied: (1) the fraction of the energy going into the electrons must be large, i.e., $\epsilon_e \to 1$, and (2) we must be in the regime of fast cooling, $\gamma_c < \gamma_m$.

In the adiabatic case, the energy E of the spherical shock is constant and is given by $E = 16\pi\gamma^2 R^3 n m_p c^2/17$ (Blandford & McKee 1976; Sari 1997). In the radiative case, the energy varies as $E \propto \gamma$, where $\gamma \cong (R/L)^{-3}$. Here $L = [17M/(16\pi m_p n)]^{1/3}$ (Blandford & McKee 1976; Vietri 1996; Katz & Piran 1997a) is the radius at which the mass swept up from the external medium equals the initial mass M of the ejecta (we used 17/16 instead of 3/4 in order to be compatible with the adiabatic expression and to enable a smooth transition between the two); we write M in terms of the initial energy of the explosion via $M = E/\gamma_0 c^2$, where γ_0 is the initial Lorentz factor of the ejecta.

In both the adiabatic and radiative cases, there is a simple relation connecting R, γ, and t: $t = R/c_t\gamma^2 c$, where the numerical value of c_t varies between ∼3 and ∼7 depending on the details of the hydrodynamic evolution and the spectrum (Sari 1997, 1998; Waxman 1997c; Panaitescu & Mészáros 1997). For simplicity, we use $t \cong R/4\gamma^2 c$ for all cases. We then have the following hydrodynamic evolution equations,

$$R(t) \cong \begin{cases} (17Et/4\pi m_p nc)^{1/4}, & \text{adiabatic}, \\ (4ct/L)^{1/7} L, & \text{radiative}, \end{cases} \tag{9}$$

$$\gamma(t) \cong \begin{cases} (17E/1024\pi n m_p c^5 t^3)^{1/8}, & \text{adiabatic}, \\ (4ct/L)^{-3/7}, & \text{radiative}. \end{cases} \tag{10}$$

Using these scalings and the results of the previous section, we can calculate the variation with time of all the relevant quantities. For an adiabatic evolution,

$$\nu_c = 2.7 \times 10^{12} \epsilon_B^{-3/2} E_{52}^{-1/2} n_1^{-1} t_d^{-1/2}\ \text{Hz},$$

$$\nu_m = 5.7 \times 10^{14} \epsilon_B^{1/2} \epsilon_e^2 E_{52}^{1/2} t_d^{-3/2}\ \text{Hz},$$

$$F_{\nu,\max} = 1.1 \times 10^5 \epsilon_B^{1/2} E_{52} n_1^{1/2} D_{28}^{-2}\ \mu\text{Jy}, \tag{11}$$

where t_d is the time in days, $E_{52} = E/10^{52}$ ergs, n_1 is n in units

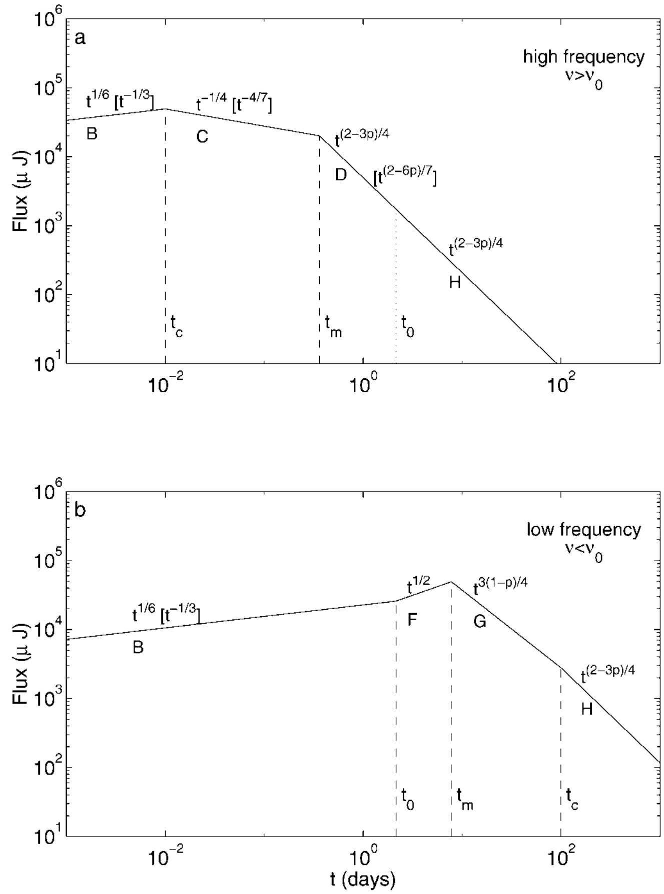

FIG. 2.—Synchrotron light curve (ignoring self-absorption). (*a*) High-frequency case ($\nu > \nu_0$). The four segments that are separated by the critical times, t_c, t_m, and t_0, correspond to the spectral segments in Fig. 1 with the same labels (B, C, D, and H). The observed flux varies with time as indicated; the scalings within square brackets are for radiative evolution (which is restricted to $t < t_0$), and the other scalings are for adiabatic evolution. (*b*) Low-frequency case ($\nu < \nu_0$).

of cm^{-3}, and $D_{28} = D/10^{28}$ cm. For a fully radiative evolution, the results are

$$\begin{aligned} \nu_c &= 1.3 \times 10^{13} \epsilon_B^{-3/2} E_{52}^{-4/7} \gamma_2^{4/7} n_1^{-13/14} t_d^{-2/7} \ \mathrm{Hz}, \\ \nu_m &= 1.2 \times 10^{14} \epsilon_B^{1/2} \epsilon_e^2 E_{52}^{4/7} \gamma_2^{-4/7} n_1^{-1/14} t_d^{-12/7} \ \mathrm{Hz}, \\ F_{\nu,\max} &= 4.5 \times 10^{3} \epsilon_B^{1/2} E_{52}^{8/7} \gamma_2^{-8/7} n_1^{5/14} D_{28}^{-2} t_d^{-3/7} \ \mu\mathrm{Jy}, \end{aligned} \tag{12}$$

where we have scaled γ_0 by a factor of 100: $\gamma_2 \equiv \gamma_0/100$.

The spectra presented in Figure 1 show ν_c and ν_m for typical parameters. In both the adiabatic and radiative cases, ν_c decreases with time slower than ν_m. Therefore, at sufficiently early times, $\nu_c < \nu_m$, i.e., fast cooling, while at later times, $\nu_c > \nu_m$, i.e., slow cooling. The transition between the two occurs when $\nu_c = \nu_m$ at t_0:

$$t_0 = \begin{cases} 210 \epsilon_B^2 \epsilon_e^2 E_{52} n_1 \ \mathrm{days}, & \text{adiabatic}, \\ 4.6 \epsilon_B^{7/5} \epsilon_e^{7/5} E_{52}^{4/5} \gamma_2^{-4/5} n_1^{3/5} \ \mathrm{days}, & \text{radiative}. \end{cases} \tag{13}$$

At $t = t_0$, the spectrum changes from fast cooling (Fig. 1*a*) to slow cooling (Fig. 1*b*). In addition, if $\epsilon_e \to 1$, the hydrodynamic evolution changes at this stage from radiative to adiabatic (see also Mészáros, Rees, & Wijers 1997). If $\epsilon_e \ll 1$, the evolution would have been adiabatic throughout. If during the fast-cooling phase ($t < t_0$) ϵ_e is somewhat less than unity, then only a fraction of the shock energy is lost to radiation. The scalings will be intermediate between the two limits of fully radiative and fully adiabatic discussed here.

During radiative evolution, the shock's energy decreases with time. When a radiative shock switches to adiabatic evolution at time $t = t_0$, it is necessary to use the reduced energy, $E_{f,52}$, to calculate the subsequent adiabatic evolution. The final energy, $E_{f,52}$, is related to the initial energy, $E_{i,52}$, of the fireball by

$$E_{f,52} = 0.022 \epsilon_B^{-3/5} \epsilon_e^{-3/5} E_{i,52}^{4/5} \gamma_2^{-4/5} n_1^{-2/5}. \tag{14}$$

Once we know how the break frequencies, ν_c and ν_m, and the peak flux, $F_{\nu,\max}$, vary with time, we can calculate the light curve. Consider a fixed frequency $\nu = 10^{15} \nu_{15}$. It follows from equations (11) and (12) that there are two critical times, t_c and t_m, when the break frequencies, ν_c and ν_m, cross the observed frequency ν:

$$t_c = \begin{cases} 7.3 \times 10^{-6} \epsilon_B^{-3} E_{52}^{-1} n_1^{-2} \nu_{15}^{-2} \ \mathrm{days}, & \text{adiabatic}, \\ 2.7 \times 10^{-7} \epsilon_B^{-21/4} E_{52}^{-2} \gamma_2^{2} n_1^{-13/4} \nu_{15}^{-7/2} \ \mathrm{days}, & \text{radiative}, \end{cases} \tag{15}$$

$$t_m = \begin{cases} 0.69 \epsilon_B^{1/3} \epsilon_e^{4/3} E_{52}^{1/3} \nu_{15}^{-2/3} \ \mathrm{days}, & \text{adiabatic}, \\ 0.29 \epsilon_B^{7/24} \epsilon_e^{7/6} E_{52}^{1/3} \gamma_2^{-1/3} \nu_{15}^{-7/12} n_1^{-1/24} \ \mathrm{days}, & \text{radiative}. \end{cases} \tag{16}$$

There are only two possible orderings of t_c, t_m, and t_0, namely, $t_0 > t_m > t_c$ and $t_0 < t_m < t_c$. We define the critical frequency, $\nu_0 = \nu_c(t_0) = \nu_m(t_0)$:

$$\nu_0 = \begin{cases} 1.8 \times 10^{11} \epsilon_B^{-5/2} \epsilon_e^{-1} E_{52}^{-1} n_1^{-3/2} \ \mathrm{Hz}, & \text{adiabatic}, \\ 8.5 \times 10^{12} \epsilon_B^{-19/10} \epsilon_e^{-2/5} E_{52}^{-4/5} \gamma_2^{4/5} n_1^{-11/10} \ \mathrm{Hz}, & \text{radiative}. \end{cases} \tag{17}$$

When $\nu > \nu_0$, the ordering $t_0 > t_m > t_c$ applies, and we refer to the corresponding light curve as the *high-frequency light curve*. Similarly, when $\nu < \nu_0$, we have $t_0 < t_m < t_c$, and we obtain the *low-frequency light curve*.

Figure 2*a* depicts a typical high-frequency light curve. At early times, the electrons cool fast and $\nu < \nu_c < \nu_m$. Ignoring self-absorption, the situation corresponds to segment B in Figure 1, and the flux varies as $F_\nu \sim F_{\nu,\max}(\nu/\nu_c)^{1/3}$. If the evolution is adiabatic, $F_{\nu,\max}$ is constant and $F_\nu \sim t^{1/6}$. In the radiative case, $F_{\nu,\max} \sim t^{-3/7}$ and $F_\nu \sim t^{-1/3}$. Figure 2*a* also depicts the scalings in the other segments, which correspond to C, D, and H in Figure 1, and can be derived in a similar fashion. Figure 2*b* shows the low-frequency light curve, corresponding to $\nu < \nu_0$. Here there are four phases in the light curve, corresponding to segments B, F, G, and H. The time dependences of the flux are also shown.

4. DISCUSSION

The main results of this Letter are summarized in Figures 1 and 2, along with the scalings given in equations (11)–(17).

It is well known that the flux at the peak of the synchrotron spectrum is independent of time in the slow-cooling limit for adiabatic hydrodynamic evolution (Katz 1994; Mészáros & Rees 1997). We have shown in this Letter that the peak flux is constant even in the fast-cooling limit if the evolution is adiabatic. The peak frequency varies as $\nu_c \propto t^{-1/2}$ during fast cooling compared with $\nu_m \propto t^{-3/2}$ during slow cooling. This is one way of distinguishing between the two cases. For a fully radiative evolution, the peak flux decreases with time as $F_{\nu,\max} \propto t^{-3/7}$, and the peak's position varies as $\nu_c \propto t^{-2/7}$ (these results differ from those given in Katz & Piran 1997a or in Mészáros, Rees, & Wijers 1997, who considered the flux at ν_m instead of the peak flux, which is at ν_c).

Even within the adiabatic case, we find that there are two possible slopes for the decaying part of the light curve. Writing the flux as $F_\nu \sim t^{-\beta}$, the two cases give $\beta = 3p/4 - 3/4$ and $\beta = 3p/4 - 1/2$. If the physics of particle acceleration in relativistic shocks is universal in the sense that the power-law index p of the electron distribution is always the same, and if the evolution is adiabatic, then we expect always to observe one of these two values of β, which differ by 1/4. Indeed, some X-ray afterglows appear to decay with $\beta \cong 1.4$, while the optical and X-ray afterglows of GRB 970228 and GRB 970508 had $\beta \cong 1.2$ (Yoshida et al. 1998; Sokolov et al. 1997). The difference between the two values is consistent with 1/4. The corresponding value of p is ~2.6, which is a reasonable energy index for shock acceleration. If future observations of gamma-ray burst afterglows always find decays with either $\beta = 1.4$ or $\beta = 1.2$, it will be a strong confirmation of the shock model and the adiabatic assumption.

In addition to the decay of the light curve with time, we can also consider the spectral index α, defined by $F_\nu \sim \nu^{-\alpha}$. The two values of β given above for adiabatic evolution correspond to $\alpha = (p - 1)/2$ and $\alpha = p/2$, respectively. Thus, the relation between β and α in an adiabatic fireball is either $\beta = 3\alpha/2$ or $\beta = 3\alpha/2 + 1/2$. Some previous studies (Mészáros & Rees 1997; Waxman 1997a) have considered the first possibility. However, for the standard choice of parameters, namely, $n \sim 1\ \mathrm{cm}^{-3}$ (a standard interstellar medium), ϵ_e, and $\epsilon_B > 0.1$ (rough equipartition of energy between electrons and magnetic fields), the second relation holds in both the optical and X-ray bands during much of the decay. Indeed, this relation is more compatible with detailed observations of GRB 970508. In a radiative evolution, the relation is $\beta = (12\alpha - 2)/7$. Future observations should be able to distinguish between the different behaviors and determine the type of solution.

Finally, we note that in none of the cases considered does the flux rise more steeply than $t^{1/2}$ (see, however, Katz & Piran 1997b). This is a potential problem since GRB 970508 displayed a sharp rise in the optical flux just before its peak at 2 days (Sokolov et al. 1997).

This work was supported by NASA grant NAG5-3516 and a US-Israel BSF grant 95-328. Re'em Sari thanks the Clore Foundations for support.

REFERENCES

Blandford, R. D., & McKee, C. F. 1976, Phys. Fluids, 19, 1130
Cohen, E., Katz, J. I., Piran, T., Sari, R., Preece, R. D., & Band, D. L. 1997, ApJ, 488, 330
Costa, E., et al. 1997, IAU Circ. 6572
Frail, D. A., Kulkarni, S. R., Nicastro, L., Feroci, M., & Taylor, G. B. 1997, Nature, in press
Groot, P. J., et al. 1997, IAU Circ. 6584
Katz, J. I. 1994, ApJ, 422, 248
Katz, J. I., & Piran, T. 1997a, ApJ, 490, 772
———. 1997b, in Proc. Fourth Huntsville Symp. on Gamma-Ray Bursts, ed. C. A. Meegan, R. D. Preece, & T. M. Koshut (New York: AIP), in press
Mészáros, P., & Rees, M. 1997, ApJ, 476, 232
Mészáros, P., Rees, M., & Wijers, R. A. M. J. 1997, preprint (astro-ph/9709273)
Paczyński, B., & Rhoads, J. 1993, ApJ, 418, L5
Panaitescu, A., & Mészáros, P. 1997, ApJ, submitted (astro-ph/9709284)
Sari, R. 1997, ApJ, 489, L37
———. 1998, ApJ, 494, L49
Sari, R., Narayan, R., & Piran, T. 1996, ApJ, 473, 204
Sokolov, V., et al. 1997, preprint (astro-ph/9709093)
Vietri, M. 1997, ApJ, 478, L9
Wijers, R. A. M. J., Rees, M., & Mészáros, P. 1997, MNRAS, 288, L51
Waxman, E. 1997a, ApJ, 485, L5
———. 1997b, ApJ, 489, L33
———. 1997c, ApJ, 491, L19
Yoshida, A., et al. 1997, in Proc. Fourth Huntsville Symp. on Gamma-Ray Bursts, ed. C. A. Meegan, R. D. Preece, & T. M. Koshut (New York: AIP), in press